Location of a Contact Site between Actin and Myosin in the Three-Dimensional Structure of the Acto–S1 Complex†

Andrzej A. Kasprzak,* Patrick Chaussepied,‡ and Manuel F. Morales
Cardiovascular Research Institute, University of California, San Francisco, San Francisco, California 94143-0524
Received March 1, 1989; Revised Manuscript Received July 18, 1989

ABSTRACT: Using fluorescence resonance energy transfer (FRET), we measured distances from chromophores located at or near the actin-binding stretch of amino acids 633–642 of myosin subfragment 1 (S1), to five points in the acto–S1 complex. Specific labeling of this site was achieved by first attaching the desired chromophore to an "antipeptide" that by means of its charge complementarity specifically binds to this segment of S1 [Chaussepied & Morales (1988) *Proc. Natl. Acad. Sci. U.S.A. 85*, 7471] and then cross-linking the fluorescent peptide to the protein. According to this technique, antipeptides containing three different labels, viz., *N*-dansylaziridine, (iodoacetamido)fluorescein, and monobromobimane, were purified and covalently bound to S1. A second chromophoric group, required for FRET measurements, was selected in such a way as to provide a good spectral overlap with the corresponding peptide chromophore. Cys-707 (SH1) and Cys-697 (SH2) on S1 were modified by using iodoacetamido and maleimido derivatives of rhodamine, 1,N^6-ethenoadenosine 5′-diphosphate was trapped at the S1 active site with orthovanadate, Cys-374 on actin was modified with either *N*-[4-[[4-(dimethylamino)phenyl]azo]phenyl]maleimide or *N*-[[(iodoacetyl)-amino]ethyl]-5-naphthylamine-1-sulfonate, and ADP bound to F-actin was exchanged with the fluorescent etheno analogue. By use of excited-state lifetime fluorometry, the following distances from the stretch 633–642 of S1 to other points on S1 or actin have been measured: Cys-707 (S1), 50.3 Å; Cys-697 (S1), 49.4 Å; active site of S1, ≥44 Å; nucleotide binding site (actin), 41.1 Å; and Cys-374 (actin), ~53 Å. Addition of MgATP had a small effect on the distance between the peptide and Cys-707, increasing it by ~2%, while it had a more pronounced effect on the distance between the peptide and Cys-697, where an increase of 14% was observed. The effect of actin on these two distances was negligible. These data enabled us (1) to place for the first time an interprotein contact in the three-dimensional map of the acto–S1 complex, (2) to definitively exclude models of communication between the nucleotide and actin binding sites in S1 that involve direct contact or close proximity of these two loci of S1, and (3) to detect intraprotein motion in S1 induced by binding of MgATP to the protein.

The mechanism by which ATP hydrolysis is linked to a change in the spatial orientation of the head portion of myosin provides the basis for understanding the energy transduction in the actomyosin system. The importance of this mechanochemical coupling was postulated a decade ago (Morales & Botts, 1979), yet only recently has it been possible to begin to understand the underlying events at the molecular level. The major difficulty in formulating a more complete theory of energy transduction in muscle has been the unavailability of crystallographically derived high-resolution structures of the two main muscle proteins, viz., myosin and actin. Both proteins have been crystallized, however, and their X-ray structures are expected to emerge in the next several years. Meanwhile, many laboratories have used alternative approaches to obtain structural information about both proteins and their complexes. These approaches include a variety of chemical cross-linkers to detect local proximities of specific amino acids, electron microscopy, X-ray diffraction, and neutron scattering to elucidate the overall shape and to locate some functional sites on S1 and actin. Fluorescence resonance energy transfer (FRET)[1] has been used most frequently, providing information about almost 60 distances in the acto–S1 complex (Botts et al., 1984, 1989; dos Remedios et al., 1987). While rapid progress in that area is being made (Takashi & Kasprzak, 1987; Barden & dos Remedios, 1987; Kasprzak et al., 1988; Trayer & Trayer, 1988; Tao & Gong, 1988; Takashi, 1989), several important locations have yet to be ascertained. Among them is that of the contact area between actin and S1 in the acto–S1 complex. The location of this region and its behavior during ATP hydrolysis are of paramount importance in order to understand the mechanism of energy transduction in this system.

A first step in locating the actomyosin interface in the three-dimensional structure of the complex has been made by synthesizing a peptide, complementary—by means of its

† This work was supported by grants from the National Institutes of Health Program Project Grant HL-16683. P.C. was supported by a fellowship from the Muscular Dystrophy Association of America. M.F.M. is a Career Investigator of the American Heart Association.
‡ Present address: CNRS, Centre de Recherches de Biochimie Macromoléculaires, Route de Mende, BP 5051, 34033 Montpellier Cédex, France.

[1] Abbreviations: S1, myosin subfragment 1; S1(A1) or S1(A2), isoenzyme of S1 containing alkali light chain 1 or 2, respectively; 1,5-IAEDANS, *N*-[[(iodoacetyl)amino]ethyl]-5-naphthylamine-1-sulfonate; 5-IAF, 5-(iodoacetamido)fluorescein; MBB, monobromobimane; ITMR, tetramethylrhodamine 5(and 6)-(iodoacetamide); MTMR, tetramethylrhodamine 5(and 6)-maleimide; DABM, *N*-[4-[[4-(dimethylamino)phenyl]azo]phenyl]maleimide; DNZ, *N*-dansylaziridine; EDC, 1-ethyl-3-[3-(dimethylamino)propyl]carbodiimide; V_i, orthovanadate; EDTA, ethylenediaminetetraacetate; DTE, dithioerythritol; DTT, dithiothreitol; SDS, sodium dodecyl sulfate; Arg-C, endoproteinase Arg-C; SH1, Cys-707 of rabbit skeletal S1 heavy chain; SH2, Cys-697 of rabbit skeletal S1 heavy chain; HPLC, high-performance liquid chromatography; FRET, fluorescence resonance energy transfer; ε-ATP, 1,N^6-ethenoadenosine 5′-triphosphate; ε-ADP, 1,N^6-ethenoadenosine 5′-diphosphate; TES, 2-[[tris(hydroxymethyl)methyl]amino]ethanesulfonate; FDNB, 1-fluoro-2,4-dinitrobenzene; Tris, tris(hydroxymethyl)aminomethane.

0006-2960/89/0428-9230$01.50/0

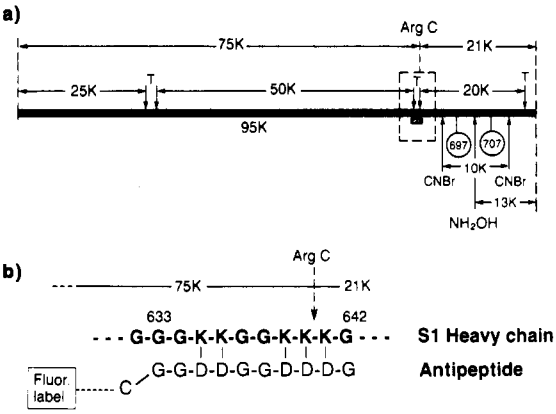

FIGURE 1: (a) Schematic representation of S1 heavy chain illustrating experimental strategy used to determine labeling specificity with the antipeptide, ITMR, and MTMR. (b) Sequence of antipeptide and its target site.

electrostatic interactions—to the part of actin binding site on S1 comprising amino acids 633–642 of the heavy chain of S1 (Chaussepied & Morales, 1988). The design of this peptide included an additional N-terminal cysteine residue (Figure 1). We have conjugated various fluorescent probes to this cysteine, producing a set of fluorescent antipeptides carrying different chromophores. Subsequently, each of these peptides was covalently attached to its target site of S1 (residues 633–642). Using FRET, we have performed distance measurements from the antipeptide to reactive thiols SH1 and SH2, to the ATPase site of S1, and—since actin still binds to the antipeptide–S1—to the nucleotide binding site and Cys-374 on actin. A preliminary report of these results has been published (Kasprzak et al., 1989).

Materials and Methods

Chemicals. DABM, 1,5-IAEDANS, ITMR, MTMR, 5-IAF, and ϵ-ATP were purchased from Molecular Probes. MBB and DNZ were obtained from Calbiochem and Pierce, respectively. L-1-(Tosylamino)-2-phenylethyl chloromethyl ketone treated trypsin and α-chymotrypsin were from Worthington, and endoproteinase Arg-C was from Boehringer Mannheim. Cyanogen bromide and EDC were supplied by Sigma. Stock solutions of sodium orthovanadate were prepared according to Goodno (1979). All other chemicals were of the highest analytical grade.

Synthesis, Labeling, and Purification of Antipeptide. The antipeptide Cys-Gly-Gly-Asp-Asp-Gly-Gly-Asp-Asp-Asp-Gly was synthesized and HPLC-purified as recently described (Chaussepied & Morales, 1988). Labeling of crude antipeptide (75–80% pure) was performed in 50 mM bicarbonate buffer, pH 9.0, at 20 °C, in the dark for 14 h, by using a 2-fold molar excess of 5-IAF or MBB or a 2.5-fold excess of DNZ. After the reaction was quenched with a 100-fold excess of β-mercaptoethanol over fluorescent dye, the sample was lyophilized and the modified antipeptide was further purified by HPLC on a Hi-pore RP318 reverse-phase column (LKB) using a gradient from 0 to 90% (v/v) of acetonitrile in 0.1% trifluoroacetic acid (the slope of the gradient was optimized for each antipeptide derivative).

The concentration of unmodified antipeptide was obtained from amino acid analysis (Chaussepied & Morales, 1988). The concentration of labeled antipeptide was measured spectrophotometrically, assuming stoichiometric modification of its N-terminal cysteine and the following extinction coefficients: $\epsilon_{495nm} = 7.2 \times 10^4$ M^{-1} cm^{-1} (pH 8.0) for IAF-P, $\epsilon_{390nm} = 5.3 \times 10^3$ M^{-1} cm^{-1} (pH 7.0) for MBB-P (Kosower et al., 1979), and $\epsilon_{327nm} = 4.7 \times 10^3$ M^{-1} cm^{-1} (pH 7.0) for DNZ-P (Deranleau & Neurath, 1963).

Proteins. Actin and myosin were prepared from rabbit skeletal muscle according to Spudich and Watt (1971) and Offer et al. (1973), respectively. Myosin subfragment 1 carrying alkali light chain 2 was isolated as described by Chaussepied and Morales (1988). Since alkali light chain 1 is cross-linked to S1 heavy chain during incubation of the A1 isozyme with EDC—an incubation necessary to prepare antipeptide–S1—only the S1(A2) isozyme was employed in the present study. Proteolyses of S1 by trypsin and by endoproteinase Arg-C were performed as previously reported (Chaussepied & Morales, 1988). CNBr and hydroxylamine cleavages of S1(A2) were conducted as described by Chaussepied et al. (1988) and by Bornstein and Balian (1977), respectively.

Preparation of Antipeptide–S1(A2) Complex. Unmodified or modified antipeptides were covalently attached to S1(A2), by using EDC catalysis, according to Chaussepied and Morales (1988), as follows. Antipeptides were cross-linked to S1(A2) (17 μM) by using 10 mM EDC in 10 mM TES buffer, pH 7.0, at 20 °C for 60 min in the dark, with an [antipeptide]:[S1] ratio of 5. The reactions were quenched by excess β-mercaptoethanol. Cross-linked protein derivatives were concentrated over Amicon PM-30 membrane and purified by Sephadex G-100 chromatography (1.5 × 20 cm column), followed by DE-52 chromatography (1.5 × 5 cm column); both columns were equilibrated with 10 mM TES and 0.1 mM NaN_3, pH 7.0. The elution of the antipeptide–S1 derivatives from the DEAE column was effected by 50 mM NaCl. After concentration as above, the complexes were dialyzed against 30 mM Tris-HCl, 0.4 mM DTE, and 0.1 mM NaN_3, pH 7.8, clarified by centrifugation for 60 min at 150000g, and finally filtered through a 0.45-μm Millipore membrane. Control, EDC-treated S1(A2) derivative was prepared by the same procedure, but without antipeptide.

Preparation of ϵ-ADP·V_i·S1(A2) Complex. ϵ-ADP·V_i was trapped at the active site of S1(A2) derivatives as described by Goodno (1979), with a slight modification. S1(A2), EDC-treated S1(A2), or antipeptide–S1(A2) complex (50 μM) was each mixed with 2 mM ϵ-ADP and 3 mM V_i in 50 mM Tris-HCl and 2.5 mM $MgCl_2$, pH 8.0, for 30 min at 20 °C in the dark. The excess free nucleotide was removed by Sephadex G-100 chromatography at 4 °C, using a 1.5 × 20 cm column equilibrated with 30 mM Tris-HCl and 0.4 mM DTE, pH 8.0. The fraction of trapped complex was evaluated by measuring the K^+/EDTA ATPase activity of S1 and assuming a linear correlation between the amount of S1-containing ϵ-ADP·V_i and the extent of K^+/EDTA ATPase inhibition (Goodno & Taylor, 1982).

Labeling of Cys-707 of S1(A2) with ITMR. Cys-707 was labeled with ITMR according to Takashi and Kasprzak (1987) with a slight modification. S1(A2) (50 μM) was incubated with a 5-fold excess of ITMR in 100 mM TES buffer and 0.3 M NaCl, pH 7.0, on ice for 2 h, in the dark. The modification was quenched by a 100-fold excess of β-mercaptoethanol over ITMR. Modified S1 was purified by gel filtration on a PD-10 column (Pharmacia) equilibrated with 10 mM TES and 0.1 mM NaN_3, pH 7.0, and then dialyzed overnight against the same buffer. The sample was then clarified by centrifugation at 160000g for 60 min and filtered through a 0.45-μm Millipore membrane. The amount of attached dye was measured spectrophotometrically by assuming $\epsilon_{555nm} = 5.0 \times 10^4$ M^{-1} cm^{-1} for S1-bound ITMR (Takashi & Kasprzak, 1987). The specificity of the labeling was verified by peptide mapping as

described elsewhere in the text.

Labeling of Cys-697 of S1(A2) with MTMR. Modification of Cys-697 was performed according to Reisler et al. (1974) and Reisler (1982), with the following modifications. S1(A2) (70–120 μM) in 0.2 M *N*-(2-hydroxyethyl)piperazine-*N*′-2-ethanesulfonate, pH 8.0, was incubated with a 5-fold molar excess of FDNB for 1 h at 0 °C. Unreacted FDNB was removed by passing the sample through a NAP-10 column (Pharmacia), equilibrated with 50 mM TES and 0.25 M NaCl, pH 7.0. To this SH1-blocked S1 was added 2.5 mM MgADP, and the mixture was incubated with a 1.75-fold molar excess of MTMR for 2 h at 0 °C. The reaction with Cys-697 was stopped and the protecting dinitrophenyl group removed from Cys-707 by adding DTT to a final concentration of 20 mM and then incubating on ice for 24 h. With Cys-707 blocked, MTMR reacts predominantly with Cys-697 of the S1 heavy chain. The only other thiol reacting with the dye is Cys-136 of the alkali light chain A2 (or Cys-177, if the A1 isozyme is used). We found that the reactivity of this cysteine toward MTMR differs slightly for the S1(A1) and S1(A2) isozymes. From quantitative fluorescence densitometry, using a Shimadzu CS 930 gel scanner, we have estimated the amount of the label in the light chain to be less than 20% for S1(A1) but less than ca. 30% for S1(A2).

Labeling of Cys-374 of actin with DABM or 1,5-IAEDANS was performed as described by Kasprzak et al. (1988). Removal of the unreacted reagent was achieved by Sephadex G-25 chromatography followed by one polymerization–depolymerization cycle. Labeled G-actin was finally polymerized with 100 mM NaCl and 2.5 mM $MgCl_2$, over 2 h at 25 °C, and the F form was kept on ice. The amount of attached DABM or 1,5-IAEDANS was estimated from absorbance, assuming $\epsilon_{460nm} = 2.48 \times 10^4$ M^{-1} cm^{-1} (Tao et al., 1983) and $\epsilon_{336nm} = 6.0 \times 10^3$ M^{-1} cm^{-1} (Hudson & Weber, 1973), respectively.

Exchange of actin-bound nucleotide with ϵ-ADP was accomplished as in Kasprzak et al. (1988).

Protein Concentrations. The concentrations of unlabeled S1(A2), EDC-treated S1(A2), and antipeptide–S1(A2) complex were measured spectrophotometrically, assuming $A^{1\%}_{280} = 7.5$ cm^{-1} (Wagner & Weeds, 1977). The concentrations of unlabeled G-actin and F-actin were measured by using $A^{1\%}_{290} = 6.3$ cm^{-1} and $A^{1\%}_{280} = 11.1$ cm^{-1}, respectively (West et al., 1967). The concentrations of labeled proteins were measured according to Bradford (1976) with the corresponding unlabeled protein as standard. Occasionally, when the concentrations of labeled proteins were measured spectrophotometrically, protein absorption was corrected for the absorption of the label at 280 or 290 nm as described earlier (Takashi & Kasprzak, 1987). Molecular weights of S1(A2) derivatives and G-actin were assumed to be 115 000 and 42 000, respectively (Margossian & Lowey, 1981; Elzinga et al., 1973).

S1(A2) ATPases. K^+/EDTA- and Ca^{2+}-dependent ATPase activities were measured at 25 °C in 50 mM Tris-HCl, pH 7.5, in the presence of 2.5 mM ATP. For K^+/EDTA ATPase this buffer was supplemented with 1 M KCl and 5 mM EDTA; for Ca^{2+} ATPase, 250 mM KCl and 5 mM $CaCl_2$ was used. The concentrations of liberated phosphate ions were measured colorimetrically according to Fiske and Subbarow.

SDS/PAGE was performed as described elsewhere (Chaussepied et al., 1986b).

Spectroscopic Measurements. Steady-state fluorescence spectra and polarization measurements were made on a three-channel SLM 8000 fluorometer. For quantum yield measurements, quinine sulfate in 0.1 N H_2SO_4 was used as a standard ($Q = 0.7$; Scott et al., 1970). To measure limiting anisotropy, the dye was first conjugated with *N*-acetyl-L-cysteine. After this product was dissolved in pure glycerol (Aldrich, spectrophotometric grade, final concentration 99.9%), the anisotropy was measured at −21 °C. To estimate depolarization caused by the local motion of the labels, the anisotropy of actin-bound labeled S1 was measured at 20 °C (Takashi & Kasprzak, 1987). A computerized Cary 118 spectrophotometer was employed to obtain absorption spectra (Takashi & Kasprzak, 1987). Fluorescence lifetimes were measured, and the Förster distances calculated as described elsewhere (Kasprzak et al., 1988). The mean lifetime of the decay, $\langle\tau\rangle$, for n fluorescent components was computed according to

$$\langle\tau\rangle = \sum_{i=1}^{n} \alpha_i \tau_i^2 / \sum_{i=1}^{n} \alpha_i \tau_i \qquad (1)$$

where α_i and τ_i denote the preexponential factor and the time constant for the ith component, respectively. For all spectroscopic measurements 30 mM Tris-HCl buffer, 2.5 mM $MgCl_2$, 0.4 mM DTE, and 0.1 mM NaN_3, pH 7.8, were used. Fluorescence spectra and lifetimes were obtained at 20 °C, with the exception of the data for ϵ-ADP trapped with V_i, where 4 °C was used.

Results and Discussion

Fluorescence Probes Can Be Specifically Placed at or near Stretch 633–642 of S1 Heavy Chain. Since our goal was to determine spatial relationship of this stretch to other loci of S1, we had to verify the validity of the method used to place chromophores at this location. The antipeptide alone has been specifically cross-linked to that part of subfragment 1 (Chaussepied & Morales, 1988). However, large and hydrophobic dyes, when conjugated with the N-terminal cysteine of the peptide, may alter or even overcome its binding specificity, which results mainly from the charge complementarity of the peptide residues to the residues of the target. To confirm the location of labeled antipeptide, we have measured the degree of protection afforded by the peptide, against Arg-C-catalyzed cleavage of the bond between Lys-640 and Lys-641 (Figure 1; Bertrand et al., 1989). It has been shown previously that there is a linear relationship between the degree of protection and the amount of the antipeptide present at its target site (Chaussepied & Morales, 1988). Using this method, we have found that in all cases ~90% of the Arg-C cleavage was inhibited, indicating that the size and nature of the fluorescence group present at the N-terminus of the peptide did not influence its binding specificity (Figure 2). In accord with this finding, in all cases the molar ratios [antipeptide]:[S1] were found to be nearly 1:1 (Table I).

The antipeptide had almost no effect on either the K^+/EDTA or Ca^+ ATPase of S1 (Table II). Most of the decrease of the K^+/EDTA activity, and the concomitant increase of the Ca^{2+} activity (Table II), can be attributed to the effect of EDC treatment on S1 (Chaussepied & Morales, 1988; Chaussepied, 1989).

Specificity of Other Labels Used. With the exception of MTMR, other modifications used in this study have been described elsewhere (see Materials and Methods) and are believed to be specific. Although the reversible protection of Cys-707 (SH1) by FDNB during Cys-697 (SH2) labeling has been known (Reisler et al., 1974), no direct evidence of the specific modification of SH2 using rhodamine derivatives has been presented. FRET measurements, reported so far, have been performed on an SH1- and SH2-modified, inactive protein. The method described in this paper (see Materials

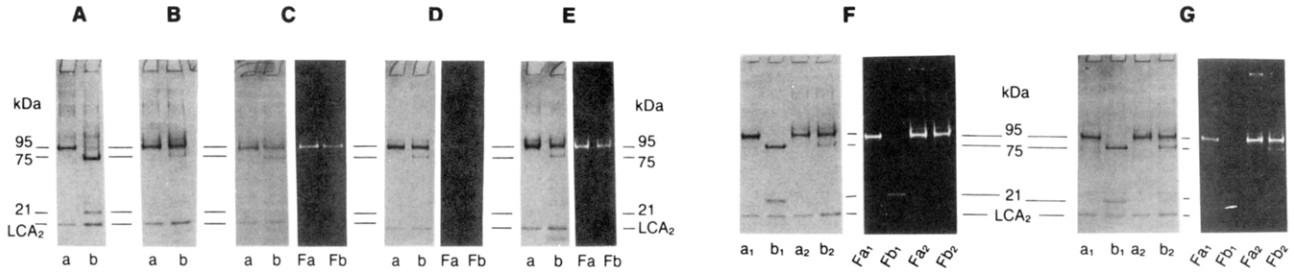

FIGURE 2: Protection of the S1(A2) heavy chain against proteolytic cleavage by endoproteinase Arg-C, observed in the presence of various antipeptides. Coomassie blue stained gels in lanes a and b were obtained without and with Arg-C, respectively; fluorescence patterns Fa and Fb, corresponding to lanes a and b, respectively, visualized under UV light. (A) control, EDC-treated S1 (no antipeptide); (B) unlabeled antipeptide; (C) DNZ–antipeptide; (D) MBB–antipeptide; (E) IAF–antipeptide; (F and G) ITMR- and MTMR- modified S1, respectively, cleaved with Arg-C, in the absence (a_1, b_1) or in the presence (a_2, b_2) of DNZ–antipeptide.

Table I: Location of Labels and Stoichiometry of Labeling

antipeptide			second label		
chromophore	[label]/[S1][a] (mol/mol)		chromophore	location	[label]/[protein][b] (mol/mol)
		Intra-S1 Distances			
DNZ	1.02	→[c]	ITMR	Cys-707	1.06
DNZ	1.05	→	MTMR	Cys-697	1.07[d]
IAF	1.13	←	ϵ-ADP·V_i	N site	0.72[e]
MBB	1.06	←	ϵ-ADP·V_i	N site	0.74[e]
		S1–Actin Distances			
MBB	1.09	←	ϵ-ADP	N site (actin)	1.00
MBB	0.96	→	DABM	Cys-374 (actin)	0.94
IAF	0.82	←	1,5-IAE-DANS	Cys-371 (actin)	1.11

[a] Moles of antipeptide-bound label per mole of S1. [b] Moles of the second label per mole of S1 for intra-S1 distances, or per mole of actin for acto–S1 distances. [c] In the donor–acceptor pairs the arrow points toward the acceptor. [d] 1.1 from absorbance measurements. [e] Based on decrease of K^+/EDTA ATPase activity.

Table II: Effect of Chemical Modification on the ATPase Activity of S1[a]

S1 derivative	K^+/EDTA activity (%)	Ca^{2+} activity (%)
S1	100[b]	100[c]
EDC–S1	69	200
P–S1	67	214
DNZ-P–S1	75	211
S1–ITMR[d]	36	305
DNZ-P–S1–ITMR[d]	26	283
S1–MTMR[e]	56	139
DNZ-P–S1–MTMR[e]	49	172
MBB-P–S1	71	205

[a] All data are for S1(A2). [b] 100% corresponds to 7.7 s^{-1}. [c] 100% corresponds to 1.8 s^{-1}. [d] ITMR conjugated with Cys-707. [e] MTMR conjugated with Cys-697.

and Methods) yields a product whose K^+/EDTA activity is reduced to approximately 50% and whose Ca^{2+} activity is elevated to ~140% of the corresponding activity for the native enzyme (Table II).

We have performed peptide mapping to localize bound MTMR. For comparative purposes and as a control on our procedures, we have also reported the data for Cys-707 (SH1) modification with ITMR (Figure 3). SDS/PAGE shows that in both cases the label was localized predominantly on the heavy chain of S1 (lanes a in Figure 3). After limited trypsinolysis the label was found in the 20k tryptic fragment of S1 (lanes b in Figure 3). Cyanogen bromide cleavage yielded a fluorescent peptide of M_r ~10K (cf. Figure 1; lanes c in Figure 3), which was previously called the "p10" peptide (Elzinga & Collins, 1977). Hydroxylamine cuts S1 heavy chain at the unique Asn–Gly bond, located between residues 698 and 699, producing a 13K peptide (Sutoh, 1981). This

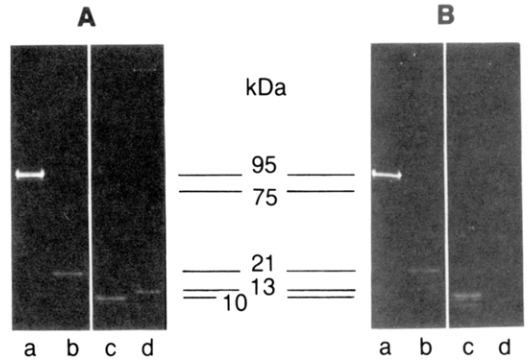

FIGURE 3: Peptide mapping of S1(A2) labeled with ITMR (A) or MTMR (B), obtained after cleaving the protein with the following reagents: (a) control (uncleaved S1); (b) trypsin; (c) cyanogen bromide; (d) hydroxylamine. See Materials and Methods for further details.

peptide was fluorescent but only if ITMR was used to label Cys-707 (see Figure 3A, lane d); no fluorescence was seen when MTMR was used to modify SH1-blocked S1 (Figure 3B, lane d). These findings agree quite well with the location of these dyes and the expected specificity of S1 thiols in reaction with ITMR and MTMR.

Antipeptide Is Useful as a Carrier of Different Chromophores for FRET Measurements. The use of an antipeptide to place chromophores in defined positions along the polypeptide chain of a protein is unprecedented. Therefore, we first discuss certain aspects of FRET measurements. In this report we used excited-state lifetimes to determine the efficiency of FRET. The advantages of utilizing lifetimes over steady-state fluorometry in FRET measurements have been discussed and documented elsewhere (Takashi & Kasprzak, 1987; Kasprzak et al., 1988). As seen from Table III, some of the donors when conjugated with S1 displayed two components in the fluorescence decay. The molecular interpretation of their occurrence is beyond the scope of this paper. It seems likely, however, that there is a single mechanism by which these components are generated. It has been suggested that the two components in the fluorescence decay of S1-bound ϵ-ADP reflect the presence of two conformational states of the protein (Rosenfeld & Taylor, 1984). On the other hand, MBB attached to the antipeptide–S1 may decay biexponentially because it senses two environments of different polarity around stretch 633–642 of S1. Since some of the donors decay monoexponentially in the absence of respective acceptors and become bi- or multiexponential in their presence, one can speculate that the reason for this behavior lies in the flexibility of the connection between the protein and the chromophore. In addition, the part of the protein to which the peptide is attached is presumably exposed and possesses several charged

Table III: Lifetime Parameters

donor–acceptor pair[a]		lifetime parameters of the donor					
		α_1	τ_1 (ns)	α_2	τ_2 (ns)	$\langle\tau\rangle$ (ns)	χ^2
DNZ-P-S1[d] (control)	DNZ-P-S1	0.450	7.87	0.550	21.15	18.06	1.40
	DNZ-P-S1 + MgATP	0.450	8.03	0.550	22.48	19.21	1.51
	DNZ-P-S1 + actin (0.94)[b]	0.502	8.99	0.498	21.55	17.84	1.39
DNZ-P-S1-ITMR (Cys-707)[d]	DNZ-P-S1-ITMR	0.707	4.93	0.293	18.54	13.22	1.82
	DNZ-P-S1-ITMR + MgATP	0.684	5.75	0.316	20.30	14.77	1.67
	DNZ-P-S1-ITMR + actin (0.79)[c]	0.698	5.37	0.302	18.00	12.85	1.96
DNZ-P-S1-MTMR (Cys-697)[d]	DNZ-P-S1-MTMR	0.704	5.45	0.296	17.96	12.71	2.17
	DNZ-P-S1-MTMR + MgATP	0.716	5.51	0.284	22.57	16.07	1.51
	DNZ-P-S1-MTMR + actin (0.82)[c]	0.705	5.18	0.295	17.50	12.40	1.87
IAF-P-S1-ϵ-*ADP·V_i*[e] or MBB-P-S1-ϵ-*ADP·V_i*[e]	P-S1-ϵ-ADP·V_i	0.501	10.52	0.499	22.99	19.06	1.37
	EDC-S1-ϵ-ADP·V_i	0.458	8.40	0.543	22.34	18.99	1.44
	IAF-P-S1-ϵ-ADP·V_i	0.526	7.70	0.474	21.95	17.95	1.35
	MBB-P-S1-ϵ-ADP·V_i	0.522	9.36	0.478	22.00	17.99	1.70
MBB-P-S1-ϵ-*ADP*-actin[e]	P-S1-ϵ-ADP-actin (0.92)[c]	1.0	28.47			28.47	1.74
	MBB-P-S1-ϵ-ADP-actin (0.85)[c]	0.403	9.74	0.597	27.44	24.02	1.27
MBB-P-S1-DABM-actin (Cys-374)[f]	MBB-P-S1-actin (0.96)[b]	0.672	8.85	0.328	18.53	13.74	1.52
	MBB-P-S1-DABM-actin (0.79)[b]	0.709	7.56	0.291	15.45	11.16	1.68
IAF-P-S1-*1,5-IAEDANS*-actin (Cys-374)[g]	P-S1-1,5-IAEDANS-actin (0.93)[c]	1.0	19.10			19.10	1.42
	IAF-P-S1-1,5-IAEDANS-actin (0.89)[c]	0.531	6.69	0.469	17.72	14.42	1.45

[a] For each donor–acceptor pair, the donor is shown in italics. [b] Molar fraction of S1 bound to actin, $[\text{acto-S1}]/[\text{S1}]_{\text{total}}$. [c] Molar fraction of actin bound to S1, $[\text{acto-S1}]/[\text{actin}]_{\text{total}}$. [d] Excited through a combination of UG1 + UG11 filters; λ_{max} = 352 nm, $\Delta\lambda(^1/_2)$ = 45 nm. [e] Excitation UG1 + UG11 filters; emission 405-nm interference filter. [f] Excitation UG1 + UG11 filters; emission combination of KV418 + BG35 + BG38 filters; λ_{max} = 432 nm, $\Delta\lambda(^1/_2)$ = 46 nm. [g] Excitation 350 nm; emission 486-nm interference filters. $\langle\tau\rangle$ has been calculated according to eq 1. For definition of χ^2 see Badea and Brand (1979).

Table IV: Spectroscopic Properties of Fluorescence Probes Bound to S1 or F-Actin[a]

probe	location	quantum yield	r_x	r_0	d_x
S1-Bound Labels					
DNZ-P	633–642	0.25	0.262[b,c]	0.336[b]	0.883
IAF-P	633–642	nd[m]	0.197[d]	0.367[d]	0.731
MBB-P	633–642	0.21	0.139[e]	0.339[e,f]	0.641
ITMR	Cys-707	nd	0.329[g]	0.375[g]	0.937
MTMR	Cys-697	nd	0.282[g]	0.375[g]	0.868
ϵ-ADP·V_i	N site	0.35[h]	nd	nd	0.806[h]
Actin-Bound Labels					
1,5-IAEDANS	Cys-374	0.63[i]	0.340[j]	0.376[j]	0.951
ϵ-ADP	N site	0.75[k]	0.234[k]	0.308[l]	0.872

[a] r_x denotes zero-time anisotropy, r_0 is the fundamental anisotropy, experimentally obtained at low temperature in the medium of high viscosity, and d_x is defined as $(r_x/r_0)^{1/2}$. [b] λ_{ex} = 340 nm, λ_{em} = 486 nm. [c] In the absence of actin r_x = 0.252. MgATP has no effect on this value. [d] λ_{ex} = 492 nm, λ_{em} = 546 nm. [e] λ_{ex} = 390 nm, λ_{em} = 480 nm. [f] A. A. Kasprzak, unpublished results. [g] λ_{ex} = 550 nm, λ_{em} = 577 nm. [h] Aguirre et al., 1989. [i] Takashi, 1979. [j] Torgerson & Morales, 1984. [k] Miki & Wahl, 1984. [l] Secrist et al., 1972. [m] nd, not determined.

groups. This creates an environment where any small change in the orientation of the dye or local protein fluctuations may produce species with distinct fluorescence characteristics. Although this complicates the interpretation of our results, the sensitivity to the molecular conformation around the antipeptide can be utilized to detect effects of ligands on the actin binding site.

To calculate the efficiency of FRET, we used the mean lifetime of the decay, defined by eq 1. The donor–acceptor distance obtained from such data has physical significance only if the separation between chromophores is unique or—in case of a distribution of donor–acceptor distances—only if such a distribution is rather narrow. In our case, the peptide can be covalently attached to S1 at five points (see Figure 1b). If the first two Lys–Asp bonds were missing, one could envision a situation in which the cysteine-conjugated chromophore would be relatively free to wobble in solution, generating a broad spectrum of distances. Such an effect is not evident, and its absence, together with the evidence that binding of the antipeptide does not induce changes in the overall structure of subfragment 1 (Chaussepied, 1989), makes the antipeptide a useful probe for FRET determination of distances in the acto-S1 complexes. However, it has to be conceded that rigorous exclusion of distance distribution would require additional analysis (Haas et al., 1975; Amir & Haas, 1987).

Spectroscopic data are presented in Tables III–VI. Table III shows our primary data concerning lifetime measurements. In Table IV, we report basic spectroscopic properties for the chromophores used, such as quantum yield and fluorescence

Table V: Overlap Integrals and Förster Critical Distances

donor–acceptor pair[a]	$J \times 10^{14}$ ($nm^4\ M^{-1}\ cm^{-1}$)	κ^2(min)	κ^2(max)	R_0(min) (Å)	$R_0(^2/_3)$ (Å)	R_0(max) (Å)
Intra-S1 Distances						
DNZ-P-S1-ITMR	14.3	0.060	3.535	28.08	41.95	55.40
DNZ-P-S1-MTMR	16.0	0.083	3.368	30.20	42.74	55.99
IAF-P-S1-ϵ-*ADP·V_i*	5.22	0.154	2.870	29.39	37.51	47.84
MBB-P-S1-ϵ-*ADP·V_i*	0.762	0.184	2.665	21.97	27.22	34.29
Actin–S1 Distances						
MBB-P-S1-ϵ-*ADP*-actin	0.782	0.163	2.792	24.53	31.04	39.41
MBB-P-S1-DABM-actin[b]	6.56	0.120	3.042	26.88	35.79	46.09
IAF-P-S1-*1,5-IAEDANS*-actin	14.8	0.106	3.179	36.22	49.22	63.86

[a] In donor–acceptor pairs the donor is shown in italics. [b] For nonfluorescent acceptors d_x of 1 was assumed.

Table VI: Energy Transfer between Chemical Points in the Acto–S1 Complex and Antipeptide-Bound Chromophores

antipeptide chromophore		second label: chromophore	second label: location	ligand	E^a (%)	R(min) (Å)	$R(^2/_3)$ (Å)	R(max) (Å)
				Intra-S1 Distances				
DNZ	→	ITMR	Cys-707	none	25.2	33.7	50.3	66.4
				MgATP	23.1	34.3	51.3	67.7
				actin	27.3	33.1	49.4	65.2
DNZ	→	MTMR	Cys-697	none	29.5	34.9	49.4	64.7
				MgATP	16.4	33.6	56.1	73.5
				actin	30.3	34.7	49.1	64.3
IAF	←	ϵ-ADP·V_i	N site	none	5.5	>47.2	>60.3	>76.8
MBB	←	ϵ-ADP·V_i	N site	none	5.6	>35.2	>43.6	>54.9
				S1–Actin Distances				
MBB	←	ϵ-ADP	N site (actin)	none	15.6	32.5	41.1[b]	52.2
MBB	→	DABM	Cys-374 (actin)	none	18.8	34.3	45.7[c]	58.8
IAF	←	1,5-IAEDANS	Cys-374 (actin)	none	24.5	43.7	59.4[d]	77.0

[a] From the average lifetimes. [b] Transfer efficiency obtained form integrated decay curve [see Kasprzak et al. (1988)] was 20.8%. Using this value and correcting for the unbound actin (Table III) yielded an $R(^2/_3)$ = 37.5 Å. [c] From integrated decay curves (see above) E = 19% and $R(^2/_3)$-(corrected) = 45.6 Å. [d] From integrated decay curve (see footnote[b]) E = 34.6% and $R(^2/_3)$ = 54.7 Å.

anisotropy, properties used later to calculate distances. Table V summarizes the values of the overlap integral, the limits of the orientation factor κ^2, and the critical Förster distances. The measured transfer efficiencies and the distances are presented in Table VI. For all measurements reported here, appropriate control experiments, intended to eliminate any nondipolar quenching contribution to FRET, were performed. Whenever actin was used, the amount of the acto–S1 complex was quantified by the cosedimentation method after spectroscopic measurements were finished; these results are reported in Table III.

The Distance from Cys-697 to the Antipeptide Increases by ~7 Å in the Presence of MgATP. Two reactive thiols of the S1 heavy chain, Cys-707 (SH1) and Cys-697 (SH2), have been the subject of numerous biochemical and biophysical studies. The sequence between and around these thiols is well conserved in myosins isolated from various organisms, which may suggest that this region of S1 has a specific but unknown function (Warrick & Spudich, 1987; Huston et al., 1988). Currently, most investigators do not consider these cysteines an essential part of the active site of myosin, and there is no strong evidence that either of them participates directly in actin binding. Our interest in these thiols stems from their possible use as indicators of structural changes and flexibility of S1 in the presence of nucleotides.

We used iodoacetamido (ITMR) and maleimido (MTMR) derivatives of rhodamine to label SH1 and SH2, respectively, and to label the peptide, we used *N*-dansylaziridine (DNZ), a thiol-specific reagent, possessing dansyl fluorescence. For DNZ (donor), rhodamine is an almost perfectly matched acceptor (Figure 4). The critical Förster distance for both pairs is approximately 42 Å (Table V), enabling accurate FRET measurements in the range 29–61 Å.

The antipeptide was found to be almost equidistant (~50 Å) from either SH1 or SH2 (Table III and VI). Actin had little effect on either distance. Addition of MgATP changed the distance of Cys-707 to the antipeptide by about 2%. In contrast, the nucleotide caused a significant, ~6.7-Å or 14%, lengthening of the interchromophore separation between Cys-697 (SH2) and the antipeptide.

We analyzed the error of the estimated distance, caused by partial labeling of light chain A2. Examination of the 3D lattice of chemical points (Botts et al., 1989) showed that the distance between Cys-136 on light chain A2 and Cys-697 on the heavy chain was approximately 60 Å. With the 42-Å Förster critical distance (Table V), the efficiency of FRET between antipeptide and a 100% labeled light chain is about

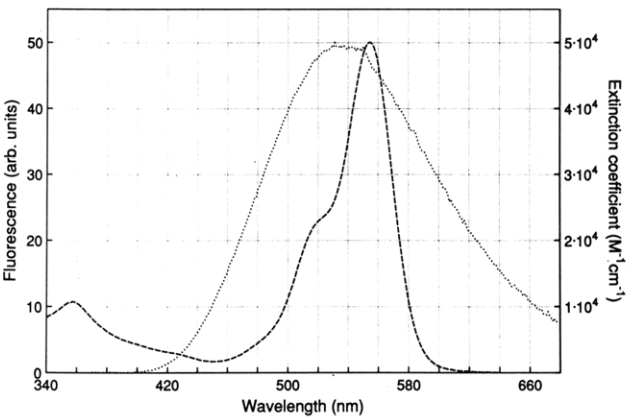

FIGURE 4: Spectral overlap of DNZ-P–S1 fluorescence (···) and MTMR–S1 absorbance (---).

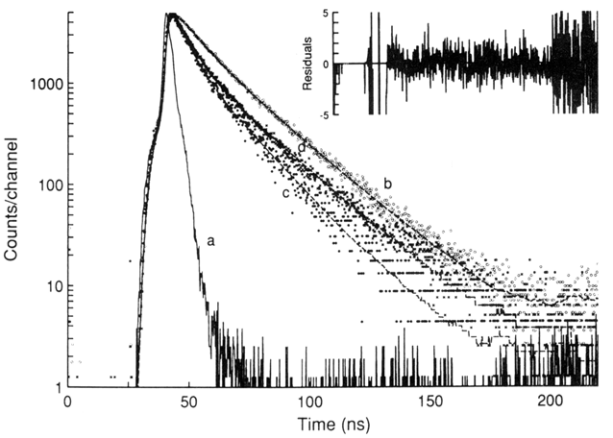

FIGURE 5: Effect of MgATP on the energy transfer between DNZ-P and MTMR, both conjugated with S1(A2). (a) Lamp profile; (b) DNZ (donor) in the absence of acceptor; (c) DNZ in the presence of acceptor (MTMR) on Cys-697; (d) as in (c) but in the presence of 1 mM MgATP. Symbols correspond to number of counts per channel; dashed lines are used for the fit. In the right-hand corner residuals for (b) were calculated as described by Grinvald and Steinberg (1974) and Badea and Brand (1979) and are shown for the full time scale of the plot (0–220 ns).

10%, and since only 30% of MTMR is on the light chain, nonspecific contributions to the mean lifetime are ~3%. This number is small, compared to the 30% FRET seen in this system.

The observed change in FRET for the transfer between DNZ and Cys-697 greatly exceeds the experimental error estimated for this kind of measurement. While some variation

of the estimated distances for other probes was seen (see below), this happened only when *different* pairs of chromophores were employed to measure the same distance. FRET measurements for the *same* donor–acceptor pair were always accurate and reproducible. Another reason for the apparent change in the transfer efficiency in this system could be large, ATP-induced alteration of the orientation factor, κ^2 in the Förster equation. This is also unlikely to take place as MgATP has no effect on the polarization of DNZ-P–S1 at room temperature (Table III). Considering these facts, we conclude that, in the presence of MgATP, the observed change in FRET corresponds to a new separation between SH2 and the stretch 633–642 of S1, and not to nonspecific labeling, trivial alteration of the orientation factor κ^2, or change of position in space of the chromophoric moieties of the probes.

Despite attention by many laboratories, well-defined alterations of S1 distances have rarely been detected. Dalbey et al. (1983) and Cheung et al. (1985) observed a decrease of about 7 Å of the SH1–SH2 distance on addition of MgATP. Recently, an attempt was made to follow the time course of this distance change (Garland et al., 1988). Our present findings corroborate these data and allow for a more precise description of this motion. The lower zero-time anisotropy values (Table IV) indicate that, in comparison with Cys-707, Cys-697 possesses a high local mobility which presumably is due to greater flexibility of the entire segment in the vicinity of this residue. Thus it is tempting to speculate that both the SH1–SH2 distance and the SH2–antipeptide distance changes occurred because SH2 (Cys-697) moved whereas Cys-707 (SH1) was motionless.

The Catalytic Site of S1 and the Antipeptide Are Separated by a Long Distance. We measured FRET between ϵ-ADP trapped with V_i and the antipeptide labeled with either monobromobimane or 5-(iodoacetamido)fluorescein (Table I). The amount of fluorescent nucleotide trapped by the protein was considerably less than stoichiometric and the ratio $[\epsilon\text{-ADP}]_{trapped}/[S1]$ was about 0.7 (Table I). We note, however, that in both FRET pairs the fluorescent nucleotide carried the *donor* chromophore. This fact makes our FRET measurements independent of the above ratio as S1 molecules that lack ϵ-ADP are not seen in these experiments. For both pairs, the transfer efficiency was ~5% (Table III). Bearing in mind that a small fraction of antipeptides may be nonspecifically bound (compare the protection of Arg-C cleavage in Figure 2), we consider the observed extent of transfer as too low for reliable estimates of the donor–acceptor separation. Consequently, in this case, the values reported in Table VI are to be taken as lower limits for this distance. For MBB-P–S1 and IAF-P–S1 the minimum distances to the active site were 43.6 and 60.3 Å, respectively (Table VI).

Many factors other than nonspecific labeling may have contributed to the disagreement between these distance estimates. (1) FRET occurs between chromophores rather than amino acids to which labels are attached. The separation between the amino acid and the chromophoric portion of the label is therefore an important factor. In the present case, the peptide-bound acceptors had different sizes. MBB is one of the smallest fluorescent probes used, whereas 5-IAF is one of the largest. Some of the divergent results obtained may be explained by this circumstance. (2) Since neither the fluorescence of the donor nor that of the acceptors is completely depolarized (Table IV), it is likely that their aromatic moieties interact with the protein. The sites of these interactions may involve different "patches" on the protein surface. Such a view is also supported by the fact that MBB is a fairly hydrophobic molecule whereas 5-IAF has several ionizable groups. (3) The acceptors may have different orientation factors. The Dale–Eisinger analysis yields a rather wide range for the absolute values of κ^2 and R_0 (Table V). The "true" value of κ^2 is, of course, unknown. If, for calculating the distance ϵ-ATP → MBB, one used the R_0(max) value rather than $R_0(^2/_3)$, a similar distance for both pairs would have been obtained. (4) Finally, we note that the peptide can be attached to S1 in two orientations, parallel, i.e., the peptide runs along the polypeptide chain of S1 in the same direction, as shown in Figure 1, and antiparallel, in which the polypeptide chain of S1 and the peptide run in opposite directions. The parallel orientation should predominate since it is stabilized by an additional electrostatic contact. However, hydrophobic interactions of the fluorescent dye with the protein may compete with the electrostatic effect, shifting the balance toward the antiparallel orientation. This effect would place the N-terminal cysteine on the peptide near residue 644 rather than in the vicinity of residue 632 (Figure 1).

Regardless of its true value, the fact that this distance is long is of great importance for the mechanism of force generation by the actomyosin system. Since the ATP molecule cannot be stretched out to cover even the shorter of the measured distances (>40 Å), we have to conclude that *the active site and the part of the actin binding site comprising residues 633–642 are spatially separated and nonoverlapping loci of the myosin head.* Hence, ATP does not exert its influence on the actomyosin interface directly but rather by transmitting it to that locus through the distortion of the intervening protein fabric.

The C-Terminal Portion of Actin Is at Least 45 Å Away from Segment 633–642 of S1. We have measured distances from the antipeptide to two loci on actin: the nucleotide binding site and Cys-374. From chemical cross-linking it has been concluded that, in the rigor complex, the N-terminal portion of actin interacts with stretches on both sides of the 50K/20K connector segment of S1 (Sutoh, 1983; Yamamoto et al., personal communication). Experiments that involve interprotein distance measurements raise the question whether the attitude of antipeptide–S1 bound to actin is approximately the same as in the complex of native proteins. In the rigor state the interaction between segment 633–642 of S1 and the N-terminal amino acids of actin does not make the most important *energetic* contribution to the stability of the complex. By blocking this interaction, K_a for actin binding to S1 decreases only by an order of magnitude (Chaussepied & Morales, 1988). In thermodynamic terms, this means that, under the experimental conditions used, stretch 633–642 contributes approximately 1.5 kcal/mol to a $\Delta G°$ of ~10 kcal/mol to the stability of the acto–S1 rigor complex. Clearly, some other interactions, unchanged by the presence of antipeptide, help to hold actin in place. Furthermore, site-specific mutagenesis of Asp-3 and Asp-11 (Solomon et al., 1988) demonstrated that these two Asp residues are relatively unimportant for S1 binding to F-actin. These results also agree with the earlier work involving antibody against this region of actin (Mêajan et al., 1986; Miller et al., 1987) and are consistent with the view that the overall spatial disposition of S1 to actin is similar in the presence and in the absence of the antipeptide.

We have measured two interprotein distances: from the antipeptide to the nucleotide binding site and to the penultimate amino acid of actin, Cys-374. The value of the latter distance was obtained for two different donor–acceptor pairs (Tables III–VI). For the distance of the antipeptide to the actin nucleotide we found a value of 41.1 Å (Table VI). There

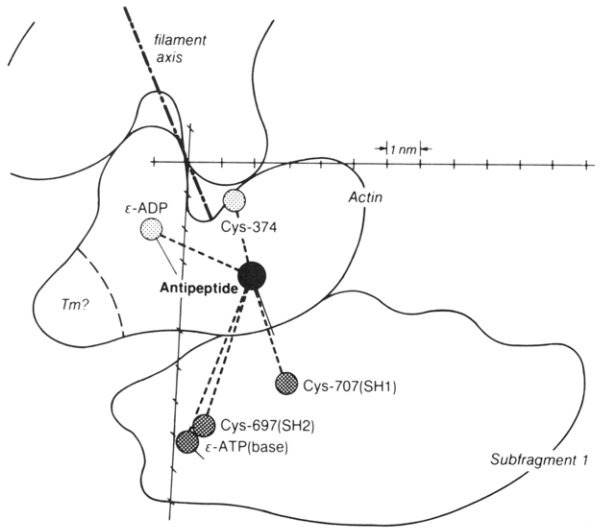

FIGURE 6: Perspective view of the S1 molecule bound to the actin filament. The z axis coincides with the filament axis; the viewer is located above the x–y plane, and the viewing angle is 15° with respect to the z axis. The contours of actin and myosin have been obtained by three-dimensional electron microscopy image reconstruction and have been reproduced from Tokunaga et al. (1987). The actomyosin contact (antipeptide) has been located by FRET as described in this paper, and its position relative to other points and to the filament axis was taken from Botts et al. (1989). A line, parallel to the filament axis, has been drawn for each point to show its distance from the plane (in the z direction). (A missing line indicates that the point lies almost in the plane.) The optimized distances, shown in the figure as dashed lines, were as follows: peptide–nucleotide (S1), 46.0 Å; peptide–Cys-707, 55.0 Å; peptide–Cys-697, 52.0 Å; peptide–nucleotide binding site (actin), 38.4 Å; and peptide–Cys-374 (actin), 58.7 Å. The scale on the axes is also shown in perspective and should not be used to compare sizes of objects located at different distances from the viewer.

is a discrepancy between the antipeptide–Cys-374 separation when two different pairs of chromophores were employed. For IAF-P(S1):1,5-IAEDANS(actin), we have obtained a distance of 59.4 Å, whereas for MBB-P(S1):DABM(actin), this distance was 45.7 Å. To explain this difference, we can apply the same arguments as to the divergent values obtained for the active site–antipeptide measurements (see above). Perhaps the average value (53 ± 10 Å) correctly represents a realistic value of the distance and its confidence limits. There are significant ramifications of this finding for the structure and organization of the protein binding sites on actin.

A number of proteins interact with two regions of actin, viz., the N-terminus (first 11 residues) and the C-terminal amino acid residues, 357–375. Sutoh and Mabuchi (1984, 1989) suggested that these two polypeptide segments of actin, albeit separated in the primary structure, are spatially close, creating a large binding site for other proteins. Since this suggestion was based on studies of the interprotein contact areas in complexes of depactin with actin, in which actin exists in its monomeric form, it is not clear if this proximity is specific for actin in its G conformation or if it should include F-actin as well. Our measurements show that even the lower value of the Cys-374–antipeptide distance (45 Å) is not short enough to support the occurrence of such proximity unambiguously. Direct FRET measurements of the separation between Cys-10 and Cys-374 on actin yielded ~32 Å (Barden & Dos Remedios, 1987). Although the specificity of Cys-10 labeling seems questionable, this distance seems to agree with our present data. In conclusion, if both termini of actin are part of a single protein–protein contact site, this site must occupy a large surface area of each protein involved. We have to remember, however, that the degree to which the antipeptide distorts the acto–S1 interface in the vicinity of its attachment site (and, therefore, the position of segment 633–641 of S1 relative the actin C-terminus) is unknown.

The Location of Antipeptide Fits Well into the 3D Lattice of Acto–S1 Points. Finally, we wished to see how the position of the antipeptide fits into the existing three-dimensional lattice of chemical points of the acto–S1 complex. For that purpose all available point-to-point distances, including measurements described above and radial distances, were used to construct a lattice, which has been subsequently optimized by using a distance geometry program (Botts et al., 1989). The optimized positions of points used in this paper were placed in the coordinate system, and an attempt was made to superpose them on the recently published contour of the acto–S1 complex (Tokunaga et al., 1987). Figure 6 shows a perspective view of this arrangement. The viewing angle is 15° with respect to the filament axis; the lines extending from the points show the vertical separation (along the z axis) for that point. As expected, the antipeptide location was found to be very near the contact area between actin and myosin. This result is not only informative but also validates our approach of using FRET for proximity mapping.

In conclusion, by applying a novel method of placing chromophores in desired positions along a polypeptide chain, we were able to determine the spatial position of the acto–S1 interface with respect to other loci of the rigor complex. The long distance between the active site and the acto–S1 contact area suggests a mechanical distortion that propagates from the S1 active site to the interface, as the means of intersite communication in the myosin head. Although neither Cys-707 nor Cys-697 is in the immediate vicinity of the interface, the nucleotide causes a significant distance lengthening between Cys-697 and the interface. We have to recall, however, that only one fragment of the acto–S1 contact areas has so far been localized, and more experimental work is needed to reveal the location of other interface points as well as to elucidate their status during ATP hydrolysis.

Acknowledgments

We thank H. C. Cheung and K. Yamamoto for making the results of their research available to us prior to publication.

Registry No. MgATP, 1476-84-2; ATPase, 9000-83-3.

References

Aguirre, R., Lin, S.-H., Gonsoulin, F., Wang, C.-K., & Cheung, H. C. (1989) *Biochemistry 28*, 799–807.

Amir, D., & Haas, E. (1987) *Biochemistry 26*, 2162–2175.

Badea, M. G., & Brand, L. (1979) *Methods Enzymol. 61*, 378–425.

Barden, J. A., & dos Remedios, C. G. (1987) *Eur. J. Biochem. 168*, 103–109.

Bertrand, R., Derancourt, J., & Kassab, R. (1989) *FEBS Lett. 246*, 171–176.

Bornstein, P., & Balian, G. (1977) *Methods Enzymol. 47*, 132–143.

Botts, J., Takashi, R., Torgerson, P., Hozumi, T., Muhlard, A., Mornet, D., & Morales, M. F. (1984) *Proc. Natl. Acad. Sci. U.S.A. 81*, 2060–2064.

Botts, J., Thomason, J. F., & Morales, M. F. (1989) *Proc. Natl. Acad. Sci. U.S.A. 89*, 2204–2208.

Bradford, M. M. (1976) *Anal. Biochem. 72*, 248–254.

Chaussepied, P. (1989) *Biochemistry* (submitted for publication).

Chaussepied, P., & Morales, M. F. (1988) *Proc. Natl. Acad. Sci. U.S.A. 85*, 7471–7475.

Chaussepied, P., Mornet, D., Barman, T. E., Travers, F., & Kassab, R. (1986a) *Biochemistry 25*, 1141–1149.

Chaussepied, P., Mornet, D., & Kassab, R. (1986b) *Proc. Natl. Acad. Sci. U.S.A. 83*, 2037–2041.
Chaussepied, P., Morales, M. F., & Kassab, R. (1988) *Biochemistry 27*, 1778–1785.
Cheung, H. C., Gonsoulin, F., & Garland, F. (1985) *Biochim. Biophys. Acta 832*, 52–62.
Dalbey, R. E., Weiel, J., & Yount, R. G. (1983) *Biochemistry 22*, 4696–4706.
Deranleau, D. A., & Neurath, H. (1966) *Biochemistry 5*, 1413.
dos Remedios, C. G., Miki, M., & Barden, J. A. (1987) *J. Muscle Res. Cell Motil. 8*, 97–117.
Elzinga, M., & Collins, J. H. (1977) *Proc. Natl. Acad. Sci. U.S.A. 74*, 4281–4284.
Elzinga, M., Collins, J. H., Kuehl, W. M., & Adelstein, R. S. (1973) *Proc. Natl. Acad. Sci. U.S.A. 70*, 2687–2691.
Garland, F., Gonsoulin, F., & Cheung, H. C. (1988) *J. Biol. Chem. 263*, 11621–11623.
Goodno, C. C. (1979) *Proc. Natl. Acad. Sci. U.S.A. 76*, 2620–2624.
Goodno, C. C., & Taylor, E. W. (1982) *Proc. Natl. Acad. Sci. U.S.A. 79*, 21–25.
Grinvald, A., & Steinberg, I. Z. (1974) *Anal. Biochem. 59*, 583–598.
Haas, E., Wilchek, M., Katchalski-Katzir, E., & Steinberg, I. Z. (1975) *Proc. Natl. Acad. Sci. U.S.A. 72*, 1807–1811.
Hudson, E. N., & Weber, G. (1973) *Biochemistry 12*, 4154–4161.
Huston, E. E., Grammer, J. C., & Yount, R. G. (1988) *Biochemistry 28*, 8945–8952.
Kasprzak, A. A., Takashi, R., & Morales, M. F. (1988) *Biochemistry 27*, 4512–4522.
Kasprzak, A. A., Chaussepied, P., & Morales, M. F. (1989) *Biophys. J. 55*, 441a.
Kosower, N. S., Kosower, E. M., Newton, G. L., & Ranney, H. M. (1979) *Proc. Natl. Acad. Sci. U.S.A. 76*, 3382–3386.
Margossian, S. S., Stafford, W. F., & Lowey, S. (1981) *Biochemistry 7*, 1214–1223.
Mējean, C., Boyer, M., Labbé, J. P., Derancourt, J., Benjamin, Y., & Roustan, C. (1986) *Biosci. Rep. 6*, 493–499.
Miki, M., & Wahl, P. (1984) *Biochim. Biophys. Acta 786*, 188–196.
Miller, L., Kalnoski, M., Yunossis, Z., Bulinsky, J. C., & Reisler, E. (1988) *Biochemistry 26*, 6064–6070.
Morales, M. F., & Botts, J. (1979) *Proc. Natl. Acad. Sci. U.S.A. 76*, 3857–3859.
Offer, G., Moss, C., & Starr, R. (1973) *J. Mol. Biol. 74*, 653–679.
Reisler, E. (1982) *Methods Enzymol. 85*, 84–93.
Reisler, E., Burke, M., & Harrington, W. F. (1974) *Biochemistry 13*, 2014–2022.
Rosenfeld, S. S., & Taylor, E. W. (1984) *J. Biol. Chem. 259*, 11908–11919.
Scott, T. G., Spencer, R. D., Leonard, N. J., & Weber, G. (1970) *J. Am. Chem. Soc. 92*, 687–695.
Secrist, J. A., III, Barrio, J. R., Leonard, N. J., & Weber, G. (1972) *Biochemistry 11*, 3499–3506.
Solomon, T. L., Solomon, L. R., Gay, L. S., & Rubenstein, P. A. (1988) *J. Biol. Chem. 263*, 19662–19669.
Spudich, J. A., & Watt, S. (1971) *J. Biol. Chem. 246*, 4866–4871.
Sutoh, K. (1981) *Biochemistry 20*, 3281–3285.
Sutoh, K. (1983) *Biochemistry 22*, 1579–1585.
Sutoh, K., & Mabuchi, I. (1986) *Biochemistry 25*, 6186–6192.
Sutoh, K., & Mabuchi, I. (1989) *Biochemistry 28*, 102–106.
Takashi, R. (1979) *Biochemistry 18*, 5164–5169.
Takashi, R. (1989) *Biophys. J. 55*, 281a.
Takashi, R., & Kasprzak, A. A. (1987) *Biochemistry 26*, 7471–7477.
Tao, T., & Gong, B.-J. (1988) *J. Cell Biol. 107*, 33a.
Tao, T., Lamkin, M., & Lehrer, S. S. (1983) *Biochemistry 22*, 3059–3064.
Tokunaga, M., Sutoh, K., Toyoshima, C., & Wakabayashi, T. (1987) *Nature 329*, 635–638.
Torgerson, P. M., & Morales, M. F. (1984) *Proc. Natl. Acad. Sci. U.S.A. 81*, 3723–3727.
Trayer, H. R., & Trayer, I. P. (1988) *Biochemistry 27*, 5718–5727.
Wagner, P. D., & Weeds, A. G. (1977) *J. Mol. Biol. 109*, 455–473.
Warrick, H. M., & Spudich, J. A. (1987) *Annu. Rev. Cell Biol. 3*, 379–421.
West, J. J., Nagy, B., & Gergely, J. (1967) *J. Biol. Chem. 242*, 1140–1145.